A computational tool for evaluating HIFU safety

Silvia Pozzi[1], Cristian Borrazzo[2], Marco Carnì[2], Elisabetta Di Castro[2], Stefano Valentini[1] and Barbara Caccia[1]

[1]*Dipartimento di Tecnologie e Salute, Istituto Superiore di Sanità, Rome, Italy*
[2]*Dipartimento di Medicina Molecolare, Sapienza Università di Roma, Rome, Italy*

Abstract
Background. High Intensity Focused Ultrasound (HIFU) is a noninvasive treatment for therapeutic applications, in particular the treatment of either benign or malignant tumor lesions. HIFU treatment is based on the power of a focused ultrasound beam to locally heat biological tissues over a necrotic level with minimal impact on the surrounding tissues. Therapies based on HIFU are becoming widely spread in the panorama of options offered by the Health Care System. Consequently, there is an ever increasing need to standardise quality assurance protocols and to develop computational tools to evaluate the output of clinical HIFU devices and ensuring safe delivery of HIFU treatment.
Aims. Goal of this study is the development of a computational tool for HIFU ablation therapy to assure safety of the patient and effectiveness of the treatment.
Results. The simulated results provide information about the behaviour of the focalized ultrasound in their interaction with different biological tissues.
Conclusions. Numerical simulation represents a useful approach to predict the heath deposition and, consequently, to assess the safety and effectiveness of HIFU devices.

Key words
• computational techniques
• medical physics
• high-intensity focused ultrasound

ORIGINAL ARTICLES AND REVIEWS

INTRODUCTION

Ultrasound is one of the most commonly used medical imaging modalities, moreover it offers an enormous potential for image-guided therapy [1]. One of the first experience, more than 50 years ago, into the use of ultrasound for medical therapy, was based on the use of focalized ultrasound as an alternative method of neurosurgery for patients with Parkinson's disease [2]. Recently High Intensity Focused Ultrasound (HIFU) is being actively investigated for use in the clinic with the aim of enabling thermal ablation of both benign and malignant tumour lesions, and bone metastasis [3-5], also associated to external radiation therapy [6], for neurosurgery [7] and drug delivery [8, 9]. HIFU ablation treatments are becoming widely spread in the panorama of options offered by the Italian Health Care System and it is particularly promising in the treatment of prostate cancer currently treated through prostatectomy [10].

HIFU ablation treatment is based on the power of a focused ultrasound beam to locally heat biological tissues over a necrotic level (to above 55-60 °C in about 3 s) with minimal impact on the surrounding tissues. A HIFU treatment can be delivered non-invasively using extracorporeal devices or minimally invasively using intracavitary or intraoperative devices. HIFU is usually delivered under either magnetic resonance (MR) or diagnostic ultrasound imaging guidance. Diagnostic ultrasound imaging is cheaper to implement and more portable, but the development of MR monitoring and temperature measurement (thermometry) techniques is more advanced. Magnetic Resonance guided Focused Ultrasound Surgery (MRgFUS) allows for both target localization and *in vivo* real time monitoring of temperature in the target through the Proton Resonance Frequency shift method (PRF) [11].

HIFU ablation therapy is usually carried out in a single session, often as a day-case procedure, with the patient either fully conscious, lightly sedated, or under general anaesthesia. It has also the advantage that it can be applied for the ablation of tumours impossible to be removed surgically, and to patients not suitable for the general anaesthesia that is required for surgery. Thus it may lead to a sensible reduction of social and economic costs. However, the application of HIFU can be compromised by the presence of sensitive normal tissues on the beam path or dangerously close to the target region. Possible burns should be avoided especially in organs like intestine, where a damage to organ walls could be lethal. Bone and scar tissues have large absorption coefficients, thus an excess of energy can be painful for the patient. Nerves can be injured by sound beams diffracted and reflected from bones [12]. Gas/liquid interfaces determine large echoes, thus organs like intestine or bladder

Address for correspondence: Barbara Caccia, Dipartimento Tecnologie e Salute, Istituto Superiore di Sanità, Viale Regina Elena 299, 00161 Rome, Italy. E-mail: barbara.caccia@iss.it.

should also be avoided to prevent damages to the beam source. Hence the support of a numerical simulation can improve the safety and effectiveness of the treatment and the comfort of the patients, and help to decrease the probability of the mentioned side effects. Consequently, there is an ever increasing need to standardise quality assurance protocols and to develop computational tools to evaluate the output of clinical HIFU devices and ensuring safe delivery of HIFU treatment [13].

In order to simulate HIFU clinical treatments, a software package to evaluate the heat deposition in an heterogeneous phantom has been developed. This work is based on a master's thesis carried out at Istituto Superiore di Sanità [14]. It is intended as a preliminary step toward the simulation of more realistic scenarios for clinical applications of HIFU treatments. The developed package allows to simulate the thermal dose distributions and could represent a tool for a quality assurance system in clinical HIFU application.

MATERIAL AND METHODS

In this work we extended the HIFU Simulator (http://www.fda.gov/AboutFDA/CentersOffices/Officeof-MedicalProductsandTobacco/CDRH/CDRHOffices/ucm301529.htm), an algorithm implemented by J.E. Soneson [15], in order to take into account the presence of layers of different materials between the pressure source and the target region. In clinical applications of HIFU the transducer lies in degassed water and is coupled to the patient through layers of water and gel to avoid large acoustic impedance mismatch, thus large echo, and to achieve a more effective acoustic energy transport to the patient.

The package consists of two modules which solve the Khokhlov-Zabolotskaya-Kunetsov (KZK) [16, 17] and the Pennes' Bio-Heat Transfer (BHT) [18] equations. The KZK equation describes the finite-amplitude wave propagation

$$\frac{\partial P}{\partial \sigma} = \frac{1}{4G} \int \nabla_{\perp}^2 P d\tau + A \frac{\partial^2 P}{\partial \tau^2} + NP \frac{\partial P}{\partial \tau} \qquad (1)$$

where $P=p/p_0$ is the pressure normalized to the source pressure, $\sigma=z/d$ is the dimensionless axial coordinate and d the focal length; $\tau=\omega_0 t'$ is the dimensionless retarded time;

$$\nabla_{\perp}^2 = \frac{\partial^2}{\partial r^2} + \left(\frac{1}{r}\right)\frac{\partial}{\partial r}$$

is the transverse Laplacian, r is the radial coordinate normalized to the source radius; $A=\alpha \cdot d$ is the dimensionless absorption parameter, where α is the tissue-specific thermoviscous attenuation coefficient (dB m^{-1}); N is the nonlinearity parameter. The BHT equation models the temperature time evolution

$$\frac{\partial T}{\partial t} = \frac{k}{\rho c_p} \nabla^2 T - \frac{w}{\rho} T + \frac{H}{\rho c_p} \qquad (2)$$

where k is the thermal conductivity (W m^{-1}K^{-1}), c_p is the specific heat capacity (J kg^{-1}K^{-1}); w is the blood perfusion rate (kg m^{-3}s^{-1}).

Using the operator splitting, the terms of the KZK equation in eq. (1) are solved with different numerical schemes. In this way the most appropriate method can be used [19]. The linear term is solved in the frequency domain with two second-order methods: a diagonal implicit Runge-Kutta scheme in the region near the transducer surface, where the solution is rapidly oscillating, and the Crank-Nicolson scheme beyond that region. The non-linear term is solved in the time domain with an upwind/downwind method. However, in order to keep the computational load within a reasonable level, the non-linear term is not computed if the amplitude of the solution is negligibly small. From the numerical solution for the pressure P, the rate of energy transferred from the propagating pressure wave to the medium, H, is computed according to the relation H=$\alpha p_0^2 P^2/\rho c_0$, where α is the above mentioned attenuation parameter (dB m^{-1}), p_0 is the pressure generated by the source transducer (Pa), ρ is the density (kg m^{-3}) of the material, and c_0 is the small-signal sound velocity (m s^{-1}). H is then the heating source that appears in eq. (2). Since the KZK equation is based on the paraxial approximation, it models the acoustic field in positions not too close to the ultrasound source and or too far off axis [20].

The BHT equation, eq. (2), is solved with a different second-order implicit Runge-Kutta scheme [15]. The computed temperature T is then used to calculate the thermal dose [4] distribution. The simulated source is an annular axisymmetric transducer (external radius 2.5 cm, internal radius 1.5 cm) radiating a continuous wave beam of 1.5 MHz frequency, as in J.E. Soneson [15]. The source is coupled to a 5 cm thick layer of water, followed by a phantom gel object. The focal distance is 8 cm, thus 3 cm into the gel. The acoustic and thermal parameters are reported in *Table 1* (first and second column), while the sonication parameters in *Table 2*.

RESULTS AND DISCUSSION
Validation of the extended code against the HIFU simulator

A first step toward a complete validation can be a comparison of the results produced with the extended code and the HIFU Simulator. In order to validate the proposed extension of the simulation model, the water thickness has been subdivided into layers. Since there are no approximations involved, the goal is to reproduce the same results of the HIFU simulator.

Figure 1a shows the axial profiles of the heating rate H, the solid line is produced with the extended code and the dash-dot line with the HIFU Simulator. The axial profiles show a small difference at the maximum (977.5 W/cm^3 for the extended code and 965.8 W/cm^3 for the HIFU Simulator) nevertheless this discrepancy decreases while refining the computational grid, and the two peaks converge to very similar values (996.7 W/cm^3 and 996.3 W/cm^3). The positions of the peaks and their full width at half-maximum (FWHM) are in very good agreement. For the extended code the z position of the peak is 7.76 cm, while for the HIFU Simulator is 7.77 cm; the FWHM values are respectively 1.07 cm and 1.08 cm. In *Figure 1b* the comparison between the computed temperature curves is reported and *Figure 1c* shows the distributions of the lethal thermal dose threshold. The temperature curves, representing in fact

Table 1
Acoustic and thermal parameters of the materials used in the simulation

Parameters	Water [15]	Phantom Gel [15]	Gel pad	Liver [21]
Speed of sound c_0 (m s^{-1})	1482	1629	1600	1597
Mass density ρ (kg m^{-3})	1000	1000	1060	1050
Attenuation 1 MHz α (dB m^{-1} MHz^{-1})	0.217	58	68	75
Power of attenuation vs frequency curve η	2	1	1	1.5
Nonlinear parameter β	3.5	4.5	4.8	7.9
Specific heat capacity C (W m^{-1}K^{-1})	4180	4180	4180	3510
Thermal conductivity k (W m^{-1}K^{-1})	0.6	0.6	0.55	0.51
Blood perfusion rate w (kg m^{-3} s^{-1})	0	20	18	0

Table 2
Parameters of the sonication sequence

Sonication parameters [15]	
Initial pulse (s)	0.3
Additional pulses cycles	5
Duty factor (%)	20
Pulse cycle period (s)	0.5
Cool-off duration (s)	5.2

The initial 0.3 s pulse is immediately followed by 5 pulses of 0.1 s repeated at 0.5 s intervals. That is, the first exposure has a total duration of 0.4 s followed by a pause of 0.4 s. Other four cycles of 0.1 s pulses and 0.4 s pauses follow. This sequence, with a total duration of 2.8 s, is followed by 5.2 s of cooling-off so that the whole sonication is extended over an 8 seconds interval.

the time evolution of the temperature in the location where it reaches its maximum, show a good agreement during the heating and the short cooling-off steps. However a small difference is visible in the last cooling-off phase of the sonication resulting in a discrepancy of one Celsius degree: 49.5 °C (extended code) and 48.5 °C (HIFU simulator). *Figure 1 c)* shows the areas of the thermal doses for both models above the lethal threshold of 240 CEM$_{43}$. The Cumulative Equivalent Minutes at 43 °C model (CEM$_{43}$), introduced by Sapareto and Dewey [4], represents the concept of thermal isoeffect dose: a reference temperature (43 °C) has been chosen to convert all thermal exposures to *equivalent minutes* at this temperature. As shown in *Figure 1 c)* the distributions of the thermal dose above the lethal threshold have an excellent overlap on-axis around the focus (8 cm), while a little discrepancy develops on the edge of the areas at about the same distance, off-axis of about ± 0.06 cm. The maximum difference between the two contours is located about 1 cm behind the focus and is of the order of 0.01 cm.

Multi-layered model: heating rate of a heterogeneous phantom

As a further step we applied the multi-layer code to a mathematical phantom made of different equivalent tissue materials. In *Figure 2* a schematic view of the simulated multi-layer phantom is shown.

The simulated layers are 2 cm of degassed water, 2 cm of an ultrasound gel pad of the kind used in clinics for a suitable anatomical positioning of the target, a 1 cm of degassed water and a layer of liver equivalent tissue. The choice of the liver as target for our code is based on the necessity to test the model on a type of tissue of particular interest for HIFU clinical application. Liver cancer management is challenging and HIFU approach represents the only treatment modality that is completely extracorporeal. The acoustic parameters of the materials are reported in *Table 1* (first, second and fourth column). The ultrasound beam is focused at 3 cm of depth into the liver that is at 8 cm from the source. The thickness of the layers has been arbitrarily chosen for a more consistent comparison with the results discussed in the previous section.

Figure 3 shows the axial profile of the heating rate H for the heterogeneous phantom. The different absorption of every layers is clearly visible in the plot: the heating rate increases at 2 cm and 5 cm from the source,
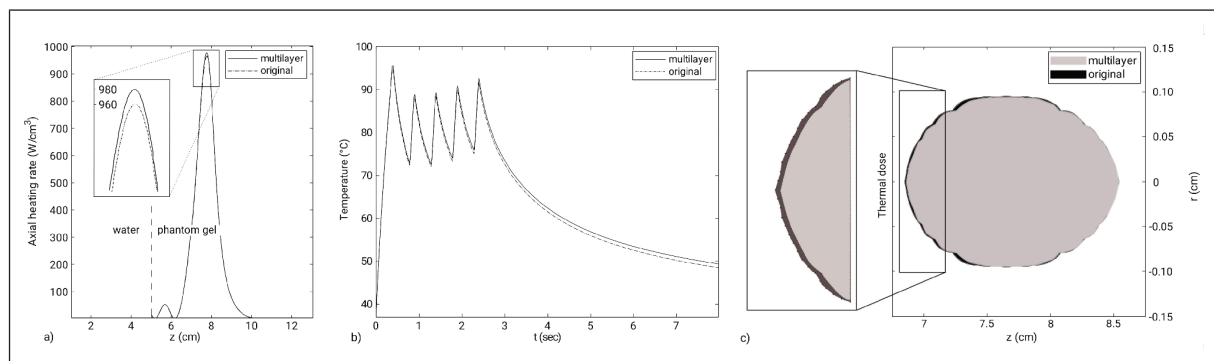

Figure 1
Comparison between the output of the KZK and BHT modules computed with the extended code (solid line) and HIFU Simulator (dash-dot line). a) Heating rate profiles; b) time evolution of the maximum temperature during one sonication; c) distributions of the thermal dose above the lethal threshold of 240 CEM$_{43}$ [4].
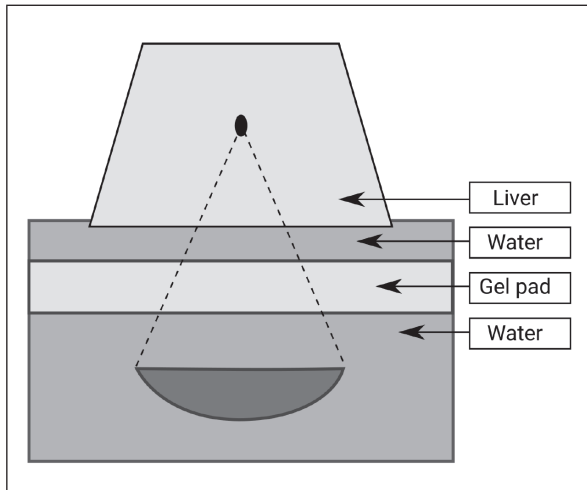
Figure 2
Schematic view of the multi-layer mathematical phantom.

Figure 3
The heating rate computed by the multi-layered model for the mathematical phantom made of four layers (2 cm of water [15], 2 cm of gel pad, 1 cm of water, and 3 cm of liver equivalent tissue [21]).

and abruptly drops at 4 cm of depth, the latter occurring when the ultrasound beam passes from a material with a high attenuation coefficient (gel) to a material with a very low one (water). Having lost energy propagating in the ultrasound gel layer, the height of the peak at focus is lower than the one simulated in the water/phantom gel body model.

DISCUSSION

The present study has developed an *in vitro* method for characterizing temporal and spatial heat generation of focused ultrasound exposures in a simple mathematical tissue-mimicking phantom. This method represents only a first step in producing a real *in vivo* simulation of the temperature variations produced by HIFU ablation therapy. Next step of this study will include the development of a mathematical tissue-mimicking phantom with different materials and including perfusion parameter values or other relevant parameters for heat deposition in biological tissues.

CONCLUSIONS

As stated in J. Civale *et al.* [13] as the use of HIFU in the clinic becomes more widespread there is an ever increasing need to standardise quality assurance protocols and calibration. This is an important aspect for a wider acceptance of HIFU as a therapeutic modality. Numerical simulation of heat propagation in different biological tissues represents a useful computational tool for dosimetry therapy planning and to simulate the behaviour of different biological tissues during the treatment. A therapy planning based on the simulation of the HIFU beam could reduce the probability of damages due to skin-burns or nerve injuries and improve the safety of the treatment.

The results obtained for the multi-layered code agree with the expected physical behaviour of ultrasound waves propagating into simulated tissues. It is the intention of the authors to further validate the model with a multi-layered phantom. This tool will be freely available through a specific section of the website of the Istituto Superiore di Sanità (http://www.iss.it/mars/).

Conflict of interest statement

There are no potential conflicts of interest or any financial or personal relationships with other people or organizations that could inappropriately bias conduct and findings of this study.

REFERENCES

1. Crum L, Bailey M, Hwang JH, Khokhlova V, Sapozhnikov O. Therapeutic ultrasound: recent trends and future perspectives. *Phys Procedia* 2010;3:25-34. DOI:10.1016/j.phpro.2010.01.005
2. Jagannathan J, Sanghvi NK, Crum LA, Yen C, Medel R, Dumont AS, Sheehan JP, Steiner L, Jolesz F, Kassell NF. High intensity focused ultrasound surgery (HIFU) of the brain: a historical perspective, with modern applications. *Neurosurgery* 2009;64(2):201-11. DOI:10.1227/01.NEU.0000336766.18197.8E
3. Mason JT. Therapeutic ultrasound an overview. *Ultrason Sonochem* 2011;18:847-52. DOI:10.1016/j.ultsonch.2011.01.004
4. Sapareto SA, Dewey WC. Thermal dose determination in cancer therapy. *Int J Radiation Oncology Biol Phys* 1984;10:787-800.
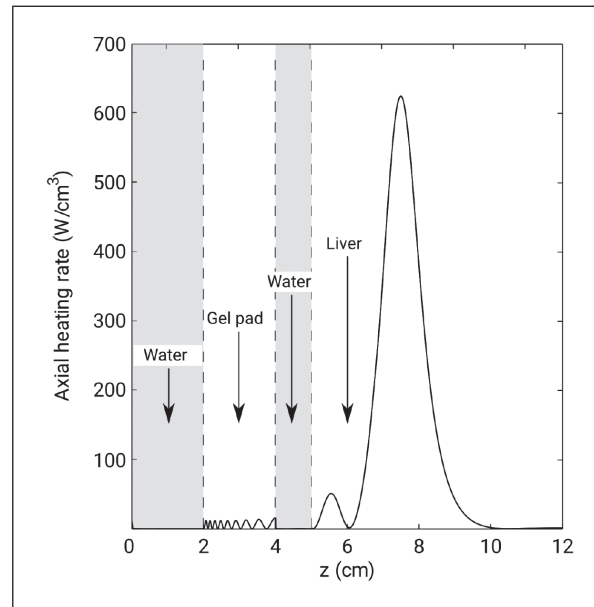
5. Dubinsky TJ, Cuevas C, Dighe MK, Kolokythas O, Hwang JH. High intensity focused ultrasound: current potential and oncologic applications. *AJR Am J Roentgenol* 2008;190:191-99. DOI:10.2214/AJR.07.2671

6. Borasi G, Russo G, Vicari F, Nahum A, Gilardi MC. Experimental evidence for the use of ultrasound to increase tumor-cell radiosensivity. *Transl Cancer Res* 2014;3(5):512-20. DOI:10.3978/j.issn.2218-676X.2014.10.05

7. Elias WJ, Huss D, Voss T, Loomba J, Khaled M, Zadicario E, Frysinger RC, Sperling SA, Wylie S, Monteith SJ, Druzgal J, Shah BB, Harrison M, Wintermark M. A pilot study of focused ultrasound thalamotomy for essential tremor. 2013 *N Engl J Med* 2013;369(7):640-8. DOI: 10.1056/NEJMoa1300962

8. Frenkel V. Ultrasound mediated delivery of drugs and genes to solid tumours. *Adv Drug Deliv Rev* 2008;60:1193-208. DOI:10.1016/j.addr.2008.03.007

9. Grull H, Langereis S. Hyperthermia-triggered drug delivery from temperature-sensitive liposomes using MRI-guided high intensity focused ultrasound. *J Control Relase* 2012;161:317-27. DOI:10.1016/j.jconrel.2012.04.041

10. Perrini MR, Migliore A, Cerbo M. HTA Report. *HIFU for the treatment of prostate cancer*. Roma: AgeNaS; 2011.

11. Schlesinger D, Benedict S, Diederich C, *et al*. MR-guided focused ultrasound surgery, present and future. *Med Phys* 2013;40:080901. DOI: 10.1118/1.4811136.

12. Hipp E, Partanen A, Karczamar GS, Fan X. Safety limitations of MR-HIFU treatment near interfaces: a phantom validation. *J Appl Clin Med Phys* 2012;13:168-75. DOI: http://dx.doi.org/10.1120/jacmp.v13i2.3739

13. Civale J, Rivens I, ter Haar G. Quality assurance for clinical high intensity focused ultrasound fields. *Int J Hyperthermia* 2015;31(2):193-202. DOI: 10.3109/02656736.2014.1002435

14. Pozzi S. *High Intensity Focused Ultrasound (HIFU): computing tools for medical applications. Thesis for Master in Scientific Computing Department of Mathematics*. Roma: Sapienza Università di Roma; 2015. (www.mat.uniroma1.it/didattica/master/vincitori-premi-finali).

15. Soneson JE. A User-Friendly Software Package for HIFU Simulation. *AIP Conf Proc* 2009;1113(165):1709-1719. DOI:10.1063/1.3131405

16. Zabolotskaya EA, Khokhlov RV. Quasi-plane waves in the nonlinear acoustics of confined beams. *Sov Phys Acoust* 1969;15:35-40.

17. Kuznetsov VP. Equations of nonlinear acoustics. *Sov Phys Acoust* 1971;16:467-70.

18. Pennes HH. Analysis of tissue and arterial blood temperatures in the resting human forearm. *J Appl Physiol* 1948;1:93-122.

19. Lee Y-S, Hamilton MF. Time-domain modeling of pulsed finite-amplitude sound beams. *J Acoust Soc Am* 1995;97:906-917. DOI: 10.1121/1.412135

20. Naze Tjotta J, Tjotta S. An analytical model for the near-field of a baffled piston transducer. *J Acoust Soc Am* 1980;68:334-9. DOI:http://dx.doi.org/10.1121/1.2017898

21. Hou GY, Luo J, Marquet F, Maleke C, Vappou J, Konofagou EE. Performance assessment of HIFU lesion detection by Harmonic Motion Imaging for focused Ultrasound (HMHIFU): A 3D finite-element-based framework with experimental validation. *Ultrasound Med Biol* 2011;37(12):2013-27. DOI:10.1016/j.ultrasmedbi.2011.09.005